Optics Communications xxx (2011) xxx–xxx

Contents lists available at ScienceDirect

Optics Communications

journal homepage: www.elsevier.com/locate/optcom

# Efficient compression of rearranged time-multiplexed elemental image arrays in MALT-based three-dimensional integral imaging

Ho-Hyun Kang [a], Byung-Gook Lee [b,*], Eun-Soo Kim [a]

[a] 3D Display Research Center, Dept. of Electronic Eng., Kwangwoon University, 447-1 Wolge-Dong, Nowon-Gu, Seoul 139-701, Republic of Korea
[b] Dept. of Visual Contents, Dongseo University, San69-1, Jurye-2Dong, Sasang-Gu, Busan 617-716, Republic of Korea

ARTICLE INFO

*Article history:*
Received 14 April 2010
Received in revised form 16 December 2010
Accepted 22 December 2010
Available online xxxx

*Keywords:*
Integral imaging
Compression
Moving array lenslet technique
Elemental images

ABSTRACT

In this paper, an approach to efficiently compress the time-multiplexed EIAs picked up from the MALT-based integral imaging system is proposed. In this method, the time-multiplexed EIAs are rearranged by collecting the elemental images occupied at the same position in each EIA to enhance the similarity among the elemental images. Then, MPEG-4 is applied to these rearranged elemental images for compression. From the experimental results, it is shown that the average correlation quality (*ACQ*) value representing a degree of similarity between the elemental images, and the resultant compression efficiency have been enhanced by 11.50% and 9.97%, respectively on the average for three kinds of test scenarios in the proposed method, compared to those of the conventional method. Good experimental results finally confirmed the feasibility of the proposed scheme.



## 1. Introduction

Since the integral imaging scheme was proposed by G. Lippmann for the first time in 1908, it has been actively researched as a promising approach for the next-generation three-dimensional (3-D) imaging and display technology because it can provide us a real 3-D image with full-parallax and continuous-viewing points [1–8].

The integral imaging system is largely composed of two parts: pickup and reconstruction. In the pickup part, direction and intensity information of rays emanating from a 3-D object are spatially sampled through a pickup lenslet array and recorded by a 2-D image sensor. Here, the recorded image data is called an elemental image array (EIA) or elemental images which represent different perspectives of a 3-D object. On the other hand, in the reconstruction part, the recorded EIA is displayed on a 2-D display panel such as the liquid crystal display (LCD), and then rays coming from the EIA are redirected through a display lenslet array to form a real 3-D image.

But, this integral imaging scheme has suffered from several drawbacks such as low resolution, narrow viewing-angle and small depth for practical applications. Especially, reconstruction of a 3-D image in high-resolution from the picked-up elemental images is highly required in most applications. The resolution of the reconstructed 3-D image might be highly dependent on the number of picked-up EIs. Therefore, the resolution of the reconstructed 3-D image can be enhanced as the number of picked-up elemental images increases.

J.-S Jang and B. Javidi proposed a concept of moving lenslet array technique (MALT) based on time-multiplexing to pick up an increased number of elemental images for resolution improvement of the reconstructed 3-D images [4]. In the MALT-based integral imaging system, the position of a pickup lenslet array is vibrated in the lateral direction to increase the spatial sampling rate, which results in a vast increase of picked-up elemental images.

Even though a significant quantity of image data can be picked up at once in the MALT-based integral imaging system for reconstruction of a high-resolution 3-D image [4,9,10], we are facing a critical issue in handling such a large data in real-time for practical purpose such as storing on a media device or transmitting through a channel. In other words, it is necessary to compress the massive data of elemental images generated from the MALT-based integral imaging system for efficient storage and transmission.

Thus far, several approaches for compression of the picked-up EIA have been presented. In 2001, M. C. Forman et al. suggested a 3-D discrete-cosine transform (DCT)-based compression method for unidirectional integral imaging [11]. In 2004, S. Yeom et al. used a video compression algorithm of MPEG-2 for data reduction of the pick-up EIA, in which elemental images were modeled as the consecutive frames in a moving picture [12]. In 2005, J.-S. Jang et al. employed the Karhunen–Loeve Transform (KLT) algorithm for compression of the picked-up EIA, in which data statistics of the elemental images was considered for compression [13]. Moreover, in 2008, H.-H. Kang proposed a sub-image array (SIA)-based compression scheme, in which the picked-up elemental images were transformed into the sub-images for improving the similarity among the sub-images and then the KLT compression algorithm was applied to these sub-images [14].

* Corresponding author. Tel.: +82 51 320 1727.
*E-mail address:* lbg@dongseo.ac.kr (B.-G. Lee).

0030-4018/$ – see front matter © 2010 Published by Elsevier B.V.
doi:10.1016/j.optcom.2010.12.076

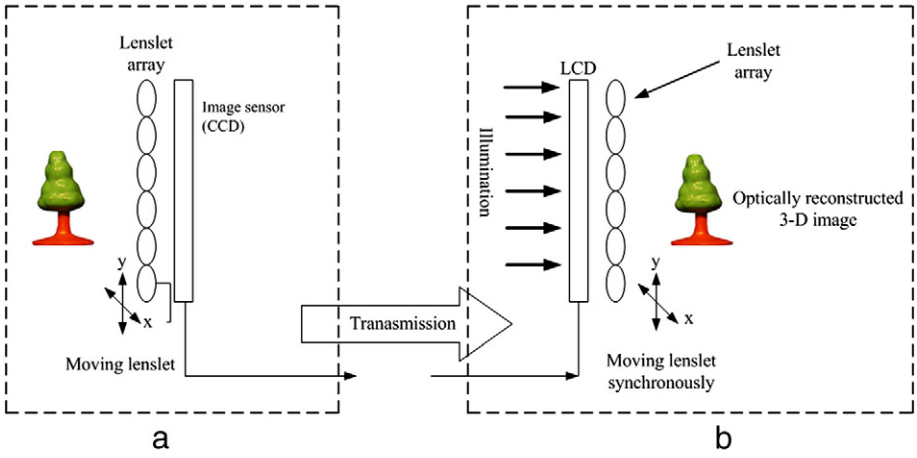


**Fig. 1.** Pickup and display setup in the MALT-based integral imaging system: (a) pickup process, and (b) display process.

In this paper, a novel approach to efficiently compress the time-multiplexed EIAs picked up from the MALT-based integral imaging system is proposed. In the proposed method, time-multiplexed EIAs are picked up with the MALT and they are rearranged by collecting the elemental images occupied at the same position in each EIA. Then, a compression algorithm of MPEG-4 is applied to these rearranged elemental images. Here, a rearrangement operation of the time-multiplexed EIAs can significantly increase the similarity among the elemental images, which may result in an increase of compression efficiency.

To show the feasibility of the proposed scheme, experiments are carried out and the results are discussed.

## 2. Review of the MALT

In general, the resolution of the reconstructed 3-D image in the integral imaging system can be determined by several system parameters including lenslet aberration, number of pixels in the image sensor and so on. Among them, one of the most fundamental factors that limit the resolution of the reconstructed 3-D image is the pitch of the lenslet arrays. This determines the ray sampling rate in the spatial dimension. From the Nyquist sampling theorem, the upper limit of the viewing resolution in the lateral direction is given by $\beta_{nyq} = l/2p$ in cycles per radian, where $p$ is the pitch of the lenslet array in the lateral direction and $l$ is the distance between the observation point and the display lenslet array [4]. To solve this limited viewing angle in the lateral direction, a concept of MALT was applied to the conventional integral imaging system.

Fig. 1 depicts the MALT-based integral imaging system. In the pickup part, the pickup lenslet array is vibrated in the lateral direction to increase the spatial sampling rate as shown in Fig. 1(a), in which the image sensor is kept to be fixed. The price we have to pay for the improved viewing-resolution in the MALT is that we have to increase the time response of the image pickup to accommodate non-stationary elemental images. For example, suppose the resolution improvement of a 3-D image $n$ times, then we should pick up the elemental images at the $n \times n$ sampling points. Here, $n = p/s$ where $s$ is the sampling interval. The pickup process is repeated within a lenslet pitch.

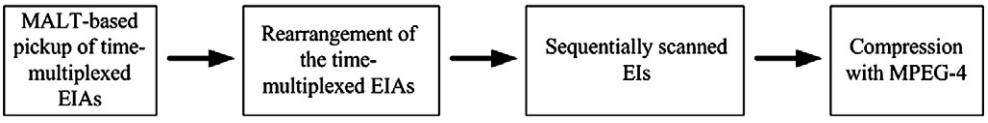


**Fig. 2.** Block diagram for compression of the rearranged time-multiplexed EIAs using MPEG-4.

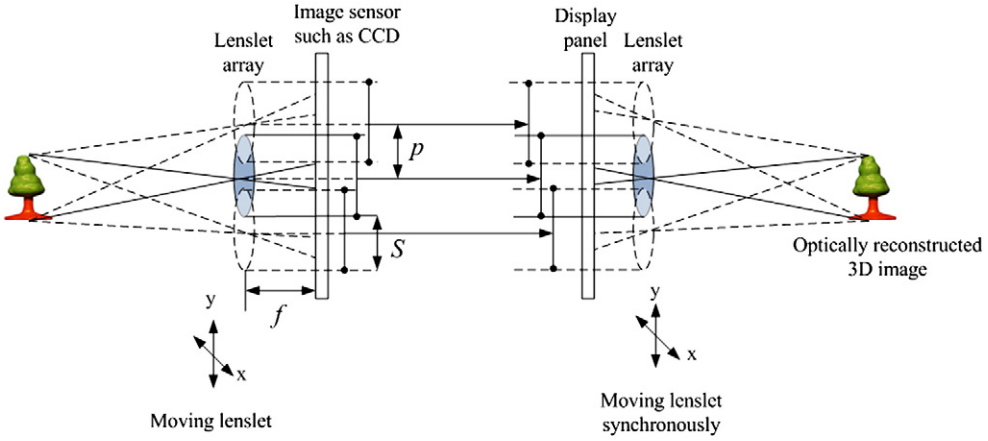


**Fig. 3.** Schematic for controlling the spatial ray sampling rate by adjusting the lenslet pitch.

Please cite this article as: H.-H. Kang, et al., Efficient compression of rearranged time-multiplexed elemental image arrays in MALT-based three-dimensional integral imaging, Opt. Commun. (2011), doi:10.1016/j.optcom.2010.12.076

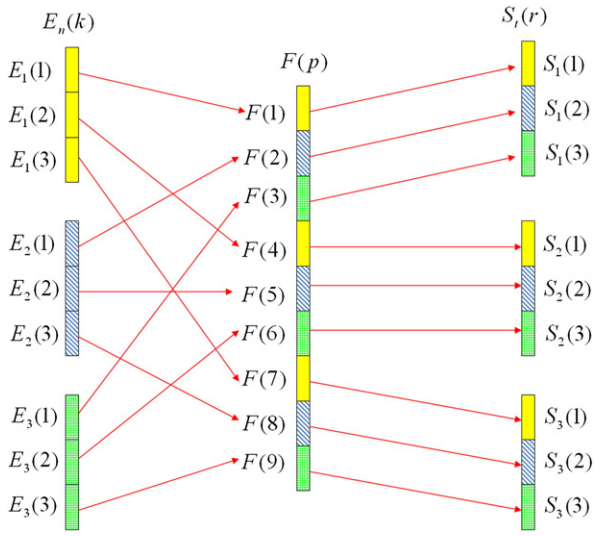


**Fig. 4.** Rearrangement process of the time-multiplexed EIAs picked-up with the MALT.

All the picked-up $n \times n$ elemental images should be transmitted to the display system through a transmission channel. Even though the resolution of the reconstructed 3-D images could be improved as the number of elemental images increases, it also causes a simultaneous increase of image data to be stored, transmitted and processed in the integral imaging system. After all, it is necessary to compress these huge data of elemental images generated from the MALT-based integral imaging system for efficient storage and transmission. For reconstruction of a 3-D image, these recorded elemental image sets are integrated in the time-domain by displaying them on the LCD at the sampling speed of the elemental images in the pickup procedure as shown in Fig. 1(b).

## 3. Proposed compression scheme

Fig. 2 shows a block diagram of the proposed compression scheme of the time-multiplexed EIAs picked up from the MALT-based integral imaging system. In this method, a set of time-multiplexed EIAs are recorded in the pickup process. Then, they are regenerated by collecting an elemental image occupied at the same position in each EIA in order to enhance their similarity for high compression. Here, the newly regenerated EIA (REIA) has a high similarity among adjacent elemental images. Next, each time-multiplexed REIA is rearranged into a one-dimensional (1-D) sequence of elemental images by using a scanning topology for compression [12]. Finally, a video compression algorithm of MPEG-4 is applied to these REIAs.

### 3.1. MALT-based pickup process

A pickup system for recording the EIA from a 3-D object is shown in Fig. 1. For pick-up of the EIA, a lenslet array is located in front of a 3-D object. Then, the EIA of the 3-D object is captured by using a CCD camera through a lenslet array.

Here, in the MALT-based pickup process, the lenslet array is vibrated in the lateral direction as shown in Fig. 3 while the image sensor is fixed. With this MALT, the spatial sampling rate can be

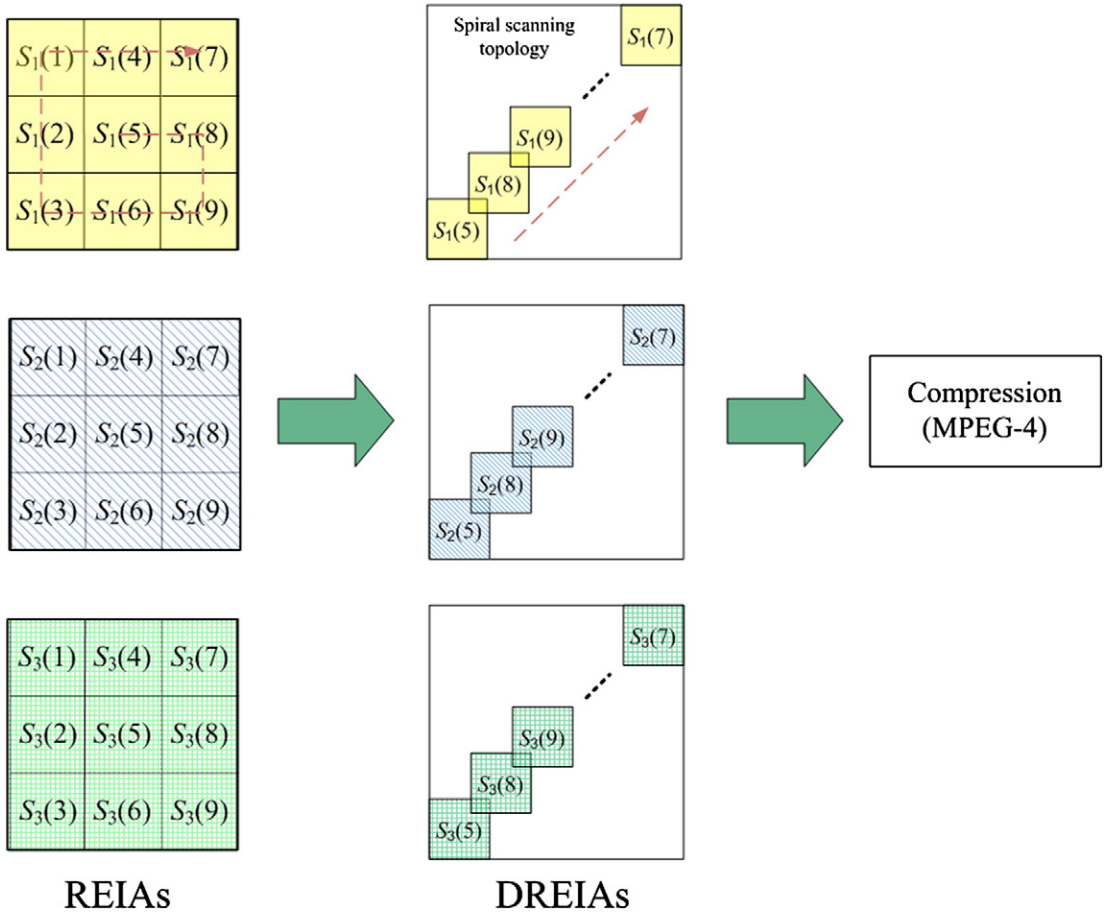


**Fig. 5.** Compression scheme of the REIAs using MPEG-4.

Please cite this article as: H.-H. Kang, et al., Efficient compression of rearranged time-multiplexed elemental image arrays in MALT-based three-dimensional integral imaging, Opt. Commun. (2011), doi:10.1016/j.optcom.2010.12.076

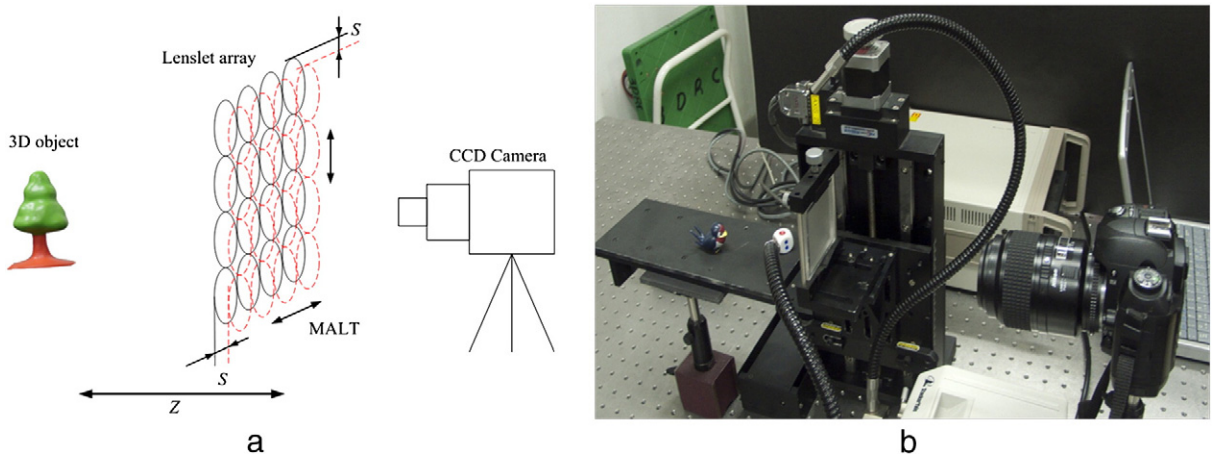


**Fig. 6.** Experimental setup for pickup of the time-multiplexed EIAs of the 3-D objects; (a) system diagram and (b) optical system.

increased by moving the sampling points of the lenslet array in the lateral direction. The movement range does not need to be larger than one pitch, because the lenslet array is periodic.

Suppose the resolution improvement of a 3-D image $n$ times, then the elemental images must be picked up at the $n \times n$ sampling points. Here, $n = p/s$ where $s$ is the sampling interval and $p$ is the pitch of the pickup lenslet array. The pickup process is repeated within a lenslet pitch and finally $n \times n$ elemental images are obtained for compression.

### 3.2. Rearrangement of EIAs picked up with the MALT

In this paper, a simple pre-process to rearrange the time-multiplexed EIAs is introduced to improve the similarity among the picked-up elemental images. A concept of rearrangement of the time-multiplexed EIAs is shown in Fig. 4. For simple explanation, suppose to pick up three EIAs placed at $x = 0$, $x = p/3$ and $x = 2p/3$ on the $x$ axis, then the three EIAs are interlaced with a ratio of 1:3 to form a new EIA. Thus, a new EIA is increased three times in size as shown in Fig. 4.

Now, consider $N$ kinds of EIAs and each EIA consists of $K$ elemental images. Here, the $k$-th elemental image of the $n$-th EIA is designated as $E_n(k)$, where $n = 1, 2, \ldots, N$ and $k = 1, 2, \ldots, K$. In case EIAs are interlaced with a ratio of 1:$N$, the new EIA denoted by $F(p)$ can be calculated by

$$F(p) = F(N \times (n-1) + k) = E_n(k). \quad (1)$$

Here, the size of the new EIA is larger by $N$ times compared to that of the original EIA. Under the same condition, this new EIA is divided into the $N$-block images which are called here the rearranged EIAs (REIAs). The $r$-th elemental image of the $t$-th REIA, which is denoted by $S_t(r)$, becomes

$$S_t(r) = F(p), \quad (2)$$

where $t = [p/N]$ and $r = p\%N$. Here, $[x]$ is the Gauss function that represents the largest integer less than or equal to the number $x$, and $a\%b$ is the remainder on division of $a$ by $b$. From Eqs. (1) and (2), we can generate the time-multiplexed REIAs from the original EIAs.

### 3.3. A sequence of elemental images and MPEG-4 algorithm

Fig. 5 shows the MPEG-4-based compression scheme of the Divided REIAs (DREIAs), in which the DREIAs represent the REIAs divided by $n \times n$ sampling points. First, each REIA can be considered as the consecutive frames in a moving picture for compression. Here we apply a spiral scanning topology to each REIA to obtain a sequence of elemental images, which is shown in Fig. 5. Basically a spiral scanning topology may be adopted in case the focused object images are mostly located around the center area of the REIA [12]. Then, a video compression algorithm of MPEG-4 is applied to these sequentially rearranged elemental images.

### 3.4. Performance evaluation parameters

To analyze the similarity of elemental images, a correlation quality ($CQ$) parameter based on normalized cross correlation is introduced. Suppose that all elemental images within either EIA or REIA are rearranged into one-dimensional elemental image sequences using a

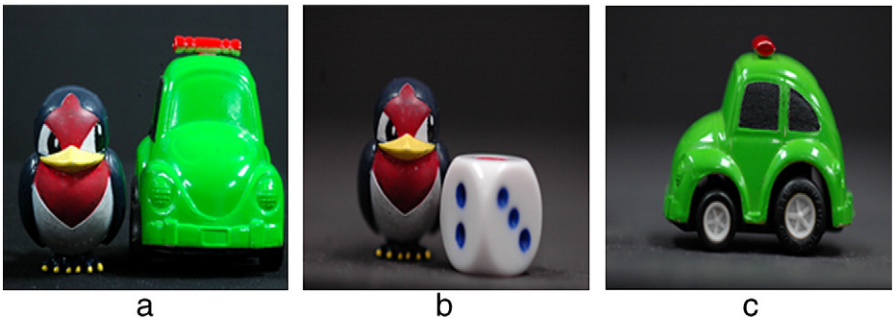


**Fig. 7.** Three kinds of 3-D object scenarios for experiments: (a) Scenario-1: two close objects of 'Bird' and 'Car', (b) Scenario-2: one close object of 'Dice' and one far object of 'Bird', and (c) Scenario-3: only one far object of 'Car'.

Please cite this article as: H.-H. Kang, et al., Efficient compression of rearranged time-multiplexed elemental image arrays in MALT-based three-dimensional integral imaging, Opt. Commun. (2011), doi:10.1016/j.optcom.2010.12.076

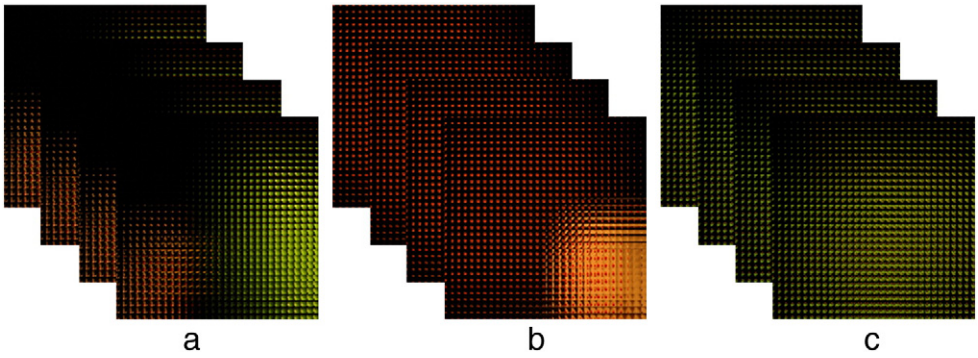


**Fig. 8.** Time-multiplexed EIAs picked up from the MALT-based system with the sampling points of 2×2: (a) for the case of Scenario-1, (b) for the case of Scenario-2, and (c) for the case of Scenario-3.

scanning algorithm for compression. We assume that two images of the sequence of elemental image sequences are $E_i$ and $E_j$ and are composed of $M\times N$ pixels. The $CQ$ between two elemental images is then defined by

$$CQ = \frac{\sum_{m=1}^{M}\sum_{n=1}^{N}\{E_i(m,n)-\bar{E}_i\}\{E_j(m,n)-\bar{E}_j\}}{\sum_{m=1}^{M}\sum_{n=1}^{N}\{E_i(m,n)-\bar{E}_i\}^2}. \quad (3)$$

Here, $m$ and $n$ are the coordinates in the elemental image. $\bar{E}_i$ and $\bar{E}_j$ are the mean values of the $E_i$ and $E_j$, respectively. The average correlation quality ($ACQ$) for the entire $P$ elemental images can be as given by

$$ACQ = \frac{1}{P}\sum_{i=1}^{P} CQ(i) = \frac{1}{P}\left[\frac{\sum_{m=1}^{M}\sum_{n=1}^{N}\{E_i(m,n)-\bar{E}_i\}\{E_j(m,n)-\bar{E}_j\}}{\sum_{m=1}^{M}\sum_{n=1}^{N}\{E_i(m,n)-\bar{E}_i\}^2}\right]. \quad (4)$$

Here, the value of $ACQ$ is normally ranged between $-1$ and $+1$, in which the value of $+1$ means two images are totally the same, and $-1$ means they are totally different. Thus, an increase of the value of ACQ implies a simultaneous increase of the similarity between two images.

To verify the quality of the encoded EIA, compression efficiency can be evaluated by two parameters. One is the compression rate ($CR$) and the other is the PSNR (peak-to-peak signal to noise ratio).

Here, the $CR$ is defined as

$$CR = \frac{Original\,image\,size}{Compressed\,image\,size}, \quad (5)$$

and the PSNR is also defined as

$$PSNR(I_o, I_u) = 10\ log_{10}\left(\frac{p_m^2}{MSE(I_o, I_u)}\right), \quad (6)$$

where $p_m$ represents the maximum value in one pixel, and $I_o$ and $I_u$ mean the original image intensity and the image intensity obtained after decompression, respectively.

Here, the mean squared error ($MSE$) is defined as

$$MSE(I_o, I_u) = \sum_{m_s=1}^{m}\sum_{n_s=1}^{n}|I_o(m_s,n_s)-I_u(m_s,n_s)|, \quad (7)$$

where $m_s$ and $n_s$ represent the pixel coordinates of $I_o$ and $I_u$, respectively.

## 4. Experiments and results

To test the proposed compression method, a set of time-multiplexed EIAs are picked up from the 3-D objects located at different locations by using the MALT-based pickup system as shown in Fig. 6 (a). The photography of the experimental setup for an optical MALT pick-up system is shown in Fig. 6(b). The lenslet array is composed of 32×32. Each lenslet element is square-shaped and has a uniform base size of 1.09×1.09 mm. The focal length of each lenslet is 3 mm. Elemental images of the 3D objects are picked up by a digital camera

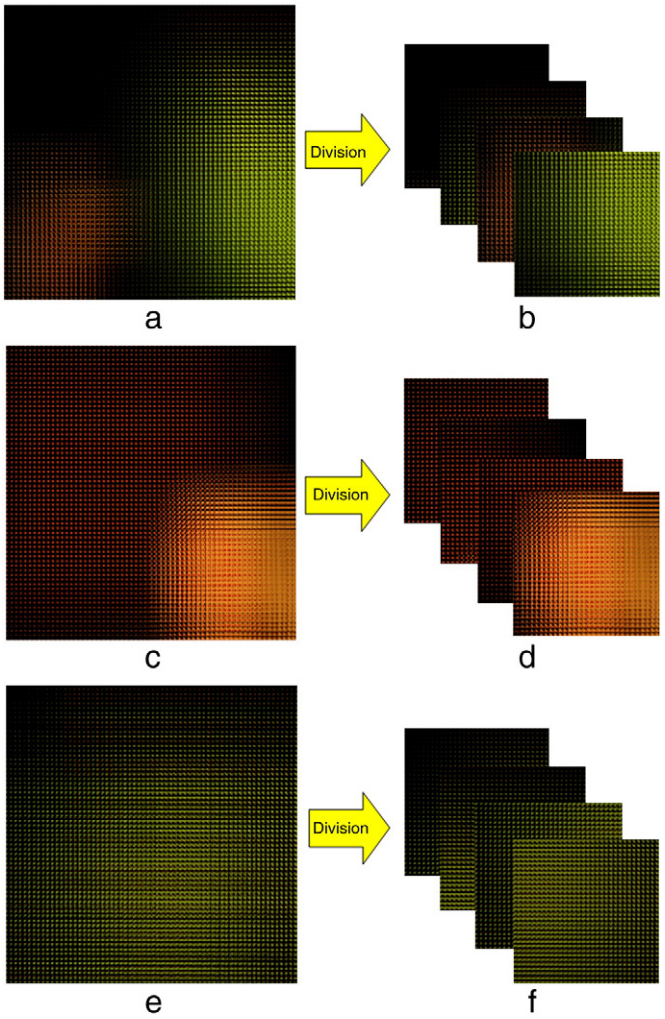


**Fig. 9.** DREIAs generated from the REIA: (a), (c) and (e) show the REIA, and (b), (d) and (f) do the DREIAs for Scenarios-1, 2 and 3, respectively.

Please cite this article as: H.-H. Kang, et al., Efficient compression of rearranged time-multiplexed elemental image arrays in MALT-based three-dimensional integral imaging, Opt. Commun. (2011), doi:10.1016/j.optcom.2010.12.076

**Table 1**
Comparison of *ACQ* values for EIAs of Fig. 8 and REIAs of Fig. 9.

| For the case of EIAs | | | For the case of DREIAs | | |
|---|---|---|---|---|---|
| Scenario-1 | Scenario-2 | Scenario-3 | Scenario-1 | Scenario-2 | Scenario-3 |
| 0.218 | −0.014 | 0.149 | 0.292 | 0.229 | 0.430 |

with a total number of $2240\times1488$ pixels where all pixels are not used. The size of each captured elemental image is 32 pixels × 32 pixels. To record $2\times2$ elemental images with MALT, we recorded each elemental image by moving the camera with the step of $p/2=1.5$ mm.

In the experiment, three 3-D objects of 'Dice', 'Bird' and 'Car' are used as the test objects, which are shown in Fig. 8. The lens array is located in front of the objects, and light passing through the lens array is captured by using a CCD camera. The size of the 'Dice', 'Bird' and 'Car' is given by $1.2\times1.2\times1.2$ cm$^3$, $2.2\times2.8\times4.5$ cm$^3$ and $3.2\times3.7\times4.7$ cm$^3$, respectively.

Fig. 7 shows three kinds of object scenarios for our experiments. In Scenario-1 of Fig. 7(a), both of the 'Bird' and 'Car' are closely located at 2 cm and 3 cm from the lenslet array, respectively. In Scenario-2 of Fig. 7(b), the 'Dice' is closely located at 1 cm, but the 'Bird' is far located at 9 cm from the lenslet array. In Scenario-3 of Fig. 7(c), only the 'Car' is far located at 9 cm from the lenslet array.

To obtain the time-multiplexed EIAs of the 3-D objects, $2\times2$ sampling points are considered in the MALT-based pick-up process of Fig. 6 and from which 4 sets of time-multiplexed EIAs are picked up for each case of Scenarios-1, 2 and 3, and they are shown in Fig. 8. Here, the pixel number of each elemental image is assumed to be $32\times32$, so that the total number of elemental images becomes 1024 $(=32\times32)$.

Then, the REIAs are generated from the originally picked-up time-multiplexed EIAs for each case of Scenarios-1, 2 and 3 by using Eqs. (1) and (2), and the results are shown in Fig. 9(a), (c) and (e). Also, the DREIAs corresponding to the REIAs are shown in Fig. 9(b), (d) and (f).

To evaluate the usefulness of the proposed method, compression experiments are carried out and the results are discussed and compared to those of the conventional method in terms of *ACQ*, *PSNR* and *CR*.

Firstly, by using Eq. (4) the *ACQ* values for the EIAs of Fig. 8 and for the DREIAs of Fig. 9 are computed, respectively. Table 1 shows the results of the calculated *ACQ* values of the EIAs and DREIAs for three cases of scenarios. Here, it must be noted that an increase of the *ACQ* value means an improvement of similarity between the elemental images. As you can see in Table 1, all *ACQ* values of the DREIAs are found to be much higher than those of the originally picked-up EIAs. That is, the *ACQ* values of the DREIAs are enhanced by 3.7%, 12.15% and 14.05% compared to those of the EIAs for each case of Scenarios-1, 2, and 3. In other words, the *ACQ* value in the proposed method is increased by 9.97% on the average compared to the conventional method. This outcome reveals that a process of rearrangement of the time-multiplexed EIAs into the REIAs in the proposed method could significantly improve the similarity among the elemental images and consequently a much enhanced compression rate is expected.

Secondly, the image quality of the decoded REIAs is evaluated in terms of *PSNR* and compared to that of the decoded EIAs. Fig. 10 shows the decoded REIAs for three cases of scenarios. Now, the *PSNR*s for the conventionally decoded EIAs and the newly decoded REIAs are calculated to be 39.55, 38.32, 38.46, and 39.92, 38.37 and 38.06, respectively for three cases of scenarios. These experimental data show that there is no big difference in the *PSNR* values between the decoded EIAs and REIAs, and confirm that the image quality of the newly decoded REIAs might be kept to be high as much as the conventionally decoded EIAs even though a high rate of compression was done in the REIAs.

Fig. 11 shows the object images computationally reconstructed on the output plane from the decoded REIAs for three kinds of scenarios. It is also validated from Fig. 11 that we can't visually find any difference in image quality between the object images reconstructed from the decoded EIAs and REIAs.

Lastly, the *CR*s for the EIAs and DREIAs are calculated and the results are shown in Table 2. Under the condition of the same value of *PSNR*, the *CR*s for each of the EIAs and DREIAs are computed with the MPEG-4 algorithm. For comparison, the *CR*s for each DREIAs are also computed with the JPEG algorithm.

As shown in Table 2, the *CR*s computed for both of the EIAs and DREIAs by using the MPEG-4 are estimated to be 31.37, 33.36, and 27.42, 29.45, and 25.24, 30.48, respectively for three cases of scenarios. Accordingly these results reveal that in the proposed compression method employing the newly generated DREIAs, compression efficiency has been improved by 6.34%, 7.40% and 20.76% compared to the conventional method using the originally picked-up EIAs.

Furthermore, in case the *CR*s of the DREIAs computed with the MPEG-4 are compared to those with the JPEG, 165% improvement of compression efficiency, on the average, has been obtained as shown in Table 2. In addition, as you can see in Table 2, all *PSNR* values of the DREIAs show more than 38 dB, which confirms that the object images reconstructed from the DREIAs could be sufficiently recognizable with a decent image quality by the human visual system [15].

Now, we performed the decoding process for compressed DREIAs. The decoding process is the inverse of the compression process. The decoded DREIA is shown in Fig. 10. To test the decoding performance, we calculated PSNR between the original images and the decoded images. The resulting PSNRs of the decoded DREIAs are 39.92, 38.37 and 38.06 compared with Fig. 9(a), (c) and (e), respectively. The decoded images were applied to 3D visualization based on the

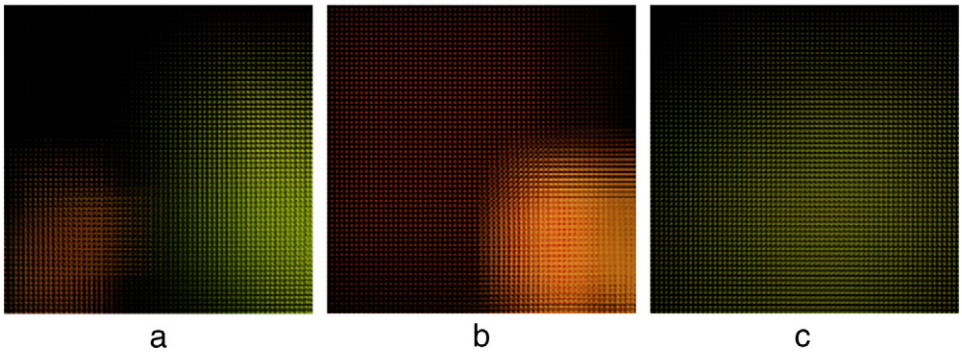


**Fig. 10.** Decoded REIAs: (a) for the case of Scenario-1 (*PSNR* = 39.92), (b) for the case of Scenario-2 (*PSNR* = 38.37), and (c) for the case of Scenario-3 (PSNR = 38.06).

Please cite this article as: H.-H. Kang, et al., Efficient compression of rearranged time-multiplexed elemental image arrays in MALT-based three-dimensional integral imaging, Opt. Commun. (2011), doi:10.1016/j.optcom.2010.12.076

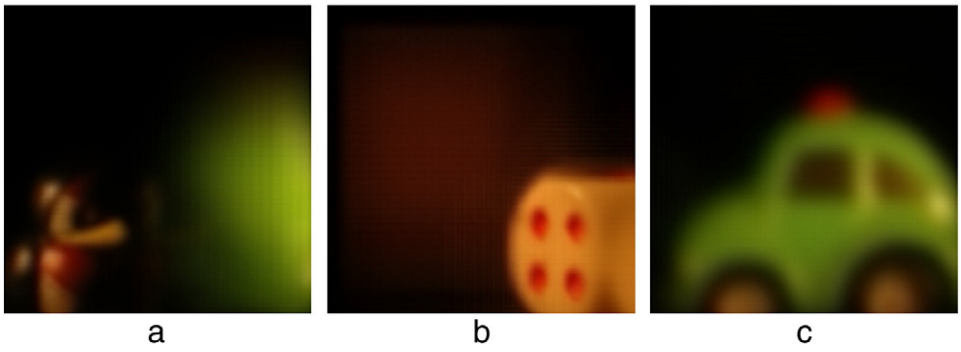


**Fig. 11.** Reconstructed 3-D object images from the decoded REIAs for three cases of the scenarios. (a) A bird and a car, (b) a dice and a bird, and (c) a car.

computational integral imaging reconstruction (CIIR). The CIIR provides 3D volumetric slice images reconstructed from the decoded images. Fig. 11 shows some examples of slice images reconstructed from three scenarios of Fig. 10.

## 5. Conclusion

In this paper, an approach to efficiently compress the time-multiplexed EIAs picked up from the MALT-based integral imaging system by employing a rearrangement process for improving the similarity between the elemental images has been proposed. Experimental results have shown that the *ACQ* value representing a degree of similarity between the elemental images and the resultant compression efficiency have been improved, on the average, by 11.50% and 9.97%, respectively in the proposed method when they are compared to those of the conventional method.

**Table 2**
Experimental results of compression ratios and PSNRs for EIAs and DREIAs.

| | | DREIAs with JPEG | EIAs with MPEG-4 | DREIAs with MPEG-4 |
|---|---|---|---|---|
| Scenario-1 | *CR* | 13.58 | 31.37 | 33.36 |
| | *PSNR* (dB) | 40.19 | 39.55 | 39.92 |
| Scenario-2 | *CR* | 10.94 | 27.42 | 29.45 |
| | *PSNR* (dB) | 38.88 | 38.21 | 38.37 |
| Scenario-3 | *CR* | 11.03 | 25.24 | 30.48 |
| | *PSNR* (dB) | 39.14 | 38.46 | 38.06 |

## Acknowledgement

This research was supported in part by the MKE (the Ministry of Knowledge Economy), Korea, under the ITRC (Information Technology Research Center) support program supervised by the NIPA (National IT Industry Promotion Agency) (NIPA-2009-C1090-0902-0018) and in part by a Research Grant 2008 from Kwangwoon University.

Byung-Gook Lee was supported by National Research Foundation of Korea Grant funded by the Korean Government (2010-0009003).

## References

[1] G. Lippmann, C.R. Acad. Sci. 146 (1908) 446.
[2] A. Stern, B. Javidi, Proc. IEEE 94 (2006) 591.
[3] B. Lee, S.Y. Jung, S.-W. Min, J.-H. Park, Opt. Lett. 26 (2001) 1481.
[4] J.-S. Jang, B. Javidi, Opt. Lett. 27 (2002) 324.
[5] M. Martínez-Corral, B. Javidi, R. Martínez-Cuenca, G. Saavedra, J. Opt. Soc. Am. A 22 (2005) 597.
[6] D.-H. Shin, S.-H. Lee, E.-S. Kim, Opt. Commun. 275 (2007) 330.
[7] J.-H. Park, K. Hong, B. Lee, Appl. Opt. 48 (2009) H77.
[8] Y. Kim, K. Hong, B. Lee, 3D Res. 01 (2010) 17.
[9] S.-H. Hong, B. Javidi, Opt. Express 12 (2004) 4579.
[10] Y.-W. Song, B. Javidi, Opt. Express 13 (2005) 3242.
[11] R. Zaharia, A. Aggoun, M. McCormick, IEEE Comput. Soc. (2001) 527, ISBN 0-7695-1031.
[12] S.-Y. Yeom, A. Stern, B. Javidi, Opt. Express 12 (2004) 1633.
[13] J.-S. Jang, S.-Y. Yeom, B. Javidi, Opt. Eng. 44 (2005) 127001.
[14] H.-H. Kang, D.-H. Shin, E.-S. Kim, Opt. Commun. 281 (2008) 3640.
[15] D.S. Taubman, M.W. Marcellin, JPEG2000—Image Compression Fundamentals, Standards and Practice, Kluwer Academic Publishers, 2002, p. 6.

Please cite this article as: H.-H. Kang, et al., Efficient compression of rearranged time-multiplexed elemental image arrays in MALT-based three-dimensional integral imaging, Opt. Commun. (2011), doi:10.1016/j.optcom.2010.12.076